

International Journal of Modern Physics E  
 © World Scientific Publishing Company

## ENERGY AND SYSTEM SIZE DEPENDENCE OF PHOTON PRODUCTION AT FORWARD RAPIDITIES AT RHIC

MONIKA SHARMA<sup>1</sup>, SUNIL DOGRA<sup>2</sup>, NEERAJ GUPTA<sup>2</sup>  
 (for the STAR Collaboration)

<sup>1</sup>*Department of Physics, Panjab University, Chandigarh - 160014, India*  
*monika@rcf.rhic.bnl.gov*

<sup>2</sup>*Department of Physics, University of Jammu, Jammu, India*  
*sunil@rcf.rhic.bnl.gov, neeraj@rcf.rhic.bnl.gov*

Received (received date)

Revised (revised date)

The energy and system size dependence of pseudorapidity ( $\eta$ ) and multiplicity distributions of photons are measured in the region  $-2.3 \leq \eta \leq -3.7$  for Cu + Cu collisions at  $\sqrt{s_{NN}} = 200$  and 62.4 GeV. Photon multiplicity measurements at forward rapidity have been carried out using a Photon Multiplicity Detector (PMD) in the STAR experiment. Photons are found to follow longitudinal scaling for Cu + Cu collisions for 0-10% centrality. A comparison of pseudorapidity distributions with HIJING model is also presented.

### 1. Introduction

One of the major goals of Relativistic Heavy Ion Collider at Brookhaven National Laboratory, Upton (NewYork), is to search for the possible formation of Quark Gluon Plasma in heavy ion collisions<sup>1</sup>. Multiplicity and pseudorapidity distributions are one of the very first measurements made at RHIC. One can obtain important information about the collision dynamics by studying dependences of the particle multiplicity and pseudorapidity distributions on collision centrality, energy, system size etc. Multiplicity distributions have been used to understand the particle production mechanism based on participant scaling, binary scaling, two component model<sup>2</sup> and recently by invoking the Color Glass Condensate (CGC)<sup>3</sup> model. Pseudorapidity distributions coupled with the measurement of average transverse energy provide information about the energy density achieved in the collision using the Bjorken formula<sup>4</sup> and on the nature of the system produced using hydrodynamics with CGC<sup>3</sup> as the initial condition.

A lot of work has been reported on measurements of the charged particles produced in heavy ion collisions covering complete pseudorapidity region<sup>5 6</sup>. But small amount of work is available for photons produced in such collisions in forward rapidity region. Only preshower detectors at Super Proton Synchrotron (SPS) and

2 *Monika Sharma, Sunil Dogra, Neeraj Gupta*

the STAR at RHIC have explored this region of pseudorapidity<sup>7,10</sup>.

Photons are considered as one of the most valuable probes of the dynamics and properties of the matter formed in the heavy ion collisions as they interact only electromagnetically<sup>10</sup>. Photons have a large mean free path and hence carry the first hand information of their origin. There are predictions of more direct photon production specifically associated to QGP formation in the heavy ion collisions<sup>11</sup>. However, the main contribution comes from the decay of  $\pi^0$ 's produced in the collisions during hadronization. Pseudorapidity distributions are used in validating the theoretical models attempting to describe the conditions in the early state of the collision<sup>12 13 9</sup>.

It has been found that at forward rapidity regions, charged particle pseudorapidity distributions show a longitudinal scaling. The variation of rapidity density per participant pair with  $(\eta - Y_{beam})$  where  $\eta$  is the pseudorapidity and  $Y_{beam}$  is the beam rapidity, is found to be independent of energy. Centrality dependence of such a behaviour has been studied by BRAHMS<sup>5</sup>, PHOBOS<sup>6</sup> and STAR<sup>7</sup>. The STAR experiment reported measurements of the pseudorapidity distribution in the forward rapidity region  $(-2.3 \leq \eta \leq -3.7)$  in Au + Au collisions at  $\sqrt{s_{NN}} = 62.4$  GeV using the preshower Photon Multiplicity Detector (PMD)<sup>9</sup>. The photon yield scales with the number of participating nucleons and follow longitudinal pseudorapidity scaling away from the mid-rapidity which is independent of energy. Limiting Fragmentation (LF) hypothesis<sup>14</sup> is used to explain this, but recently CGC<sup>3</sup> is also used to understand the effect at forward rapidities. B.B. Back *et al.*<sup>15</sup>, observed that pseudorapidity distributions of charged particles for central Au + Au and Cu + Cu collisions exhibit the same shape over six units of rapidity (i.e.,  $|\eta| < 3$ ). The ratios of  $dN_{ch}/d\eta$  between Au + Au and Cu + Cu collisions are constant at a value of 3.6 for 62.4 GeV and 3.56 for 200 GeV and are slightly more than the ratio of number of nucleons available in the initial state i.e.,  $A_{Au}/A_{Cu} = 3.13$ . For  $|\eta| > 3$  they fall off more steeply for 62.4 GeV than for 200 GeV.

In view of the above work, it is important to investigate the energy as well as system size dependence of pseudorapidity distributions of photons. In this paper, we present the pseudorapidity distributions of photons for Cu + Cu collisions at  $\sqrt{s_{NN}} = 200$  GeV and 62.4 GeV. These studies have been carried out for different collision centralities. Results have been compared with HLJING monte carlo event generator<sup>16</sup>.

## 2. Experimental Setup and Data Analysis

The PMD is placed at a Z-distance of 5.4 m from the center of TPC (the nominal collision point) along the beam axis. It consists of a highly segmented gaseous detector on a plane placed behind a lead converter plate of 3 radiation length ( $3X_0$ ) thick<sup>17</sup>, known as preshower plane. A veto plane which is also a gaseous detector is placed in front of the converter to reject the charged particles. The planes are further sub-divided into 12 gas tight entities, known as supermodules (SMs). Veto

plane is not used in this analysis. Discrimination between photons and charged hadrons is done by their difference in response e.g., charged hadrons affect mostly one cell with Minimum Ionising Particle (MIP) like energy deposition, whereas the number of cells affected and signal from photon are large.

Uniformity of the detector is obtained by finding MIP-response from each cell. MIP response of each cell is obtained by selecting cells having a signal surrounded by six cells without any signal representing an isolated cell. Fig. 1 displays the ADC distribution of an isolated cell which follows a Landau distribution with a mean of 84.61 ADC and most probable value (MPV) of 33.41 ADC. The relative gain for each cell is computed by dividing the cell ADC mean by the average mean of all cells in a SM. Fig. 2 displays a typical cell-to-cell relative gain distribution for one SM. Photons in an event are counted by finding clusters from cells with non-zero

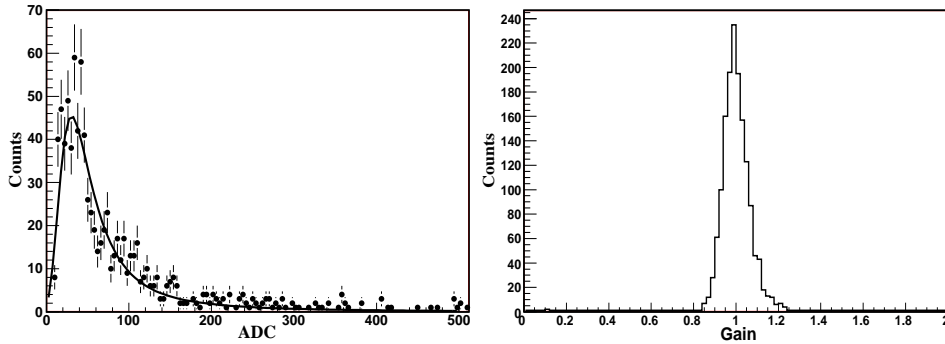


Fig. 1. ADC distribution of an isolated cell.

Fig. 2. Relative cell-to-cell gain distribution.

signal and applying a suitable cut on the cluster signal and number of cells to reject charged hadrons. Following criteria is evolved to find photon like clusters ( $N_{\gamma-like}$ ) using the HIJING Monte Carlo event generator + GEANT<sup>18</sup> : (a) the number of hit cells in a cluster  $> 1$  and (b) the cluster signal is 3 times or more than the average response of all isolated cells in a SM. Similar threshold is also applied in data to count number of photon like clusters event-by-event. The number of photons ( $N_{\gamma}$ ) from the ( $N_{\gamma-like}$ ) are obtained as :

$$N_{\gamma} = N_{\gamma-like} * \frac{f_p}{\epsilon_{\gamma}} \quad (1)$$

Simulations have been performed by running full GEANT with STAR geometry (GSTAR) using HIJING events for obtaining efficiency ( $\epsilon_{\gamma}$ ) and purity ( $f_p$ ). Photon reconstruction efficiency ( $\epsilon_{\gamma}$ ) and purity ( $f_p$ ) are calculated as :

$$\epsilon_{\gamma} = \frac{N_{cls}^{\gamma,th}}{N_{inc}^{\gamma}} \quad (2)$$

4 *Monika Sharma, Sunil Dogra, Neeraj Gupta*

$$f_p = \frac{N_{cls}^{\gamma,th}}{N_{\gamma-like}} \quad (3)$$

Here  $N_{cls}^{\gamma,th}$  is the number of photon clusters identified above the hadron rejection threshold and  $N_{inc}^{\gamma}$  are the number of incident photons. Both  $N_{cls}^{\gamma,th}$  and  $N_{inc}^{\gamma}$  are obtained from the event generator. The geometrical acceptance factors defined below are obtained pseudorapidity binwise for the SMs used in the present PMD analysis.

$$A = \frac{\text{Total cells within the pseudorapidity bin}}{\text{Total number of active cells}} \quad (4)$$

For the present analysis, we have selected SMs with stable gain throughout the data taking. Also, cells with abnormally high frequency of hits were treated as dead cells. In order to implement the SM to SM gain variation, we have calculated average MIP for each SM from data. Taking the SM with best developed MIP as standard, the variation of SM-wise gain has been incorporated in simulations and the responses of cells are changed accordingly.

### 3. Results and Discussions

The data for Cu + Cu collisions at  $\sqrt{s_{NN}} = 200$  and 62.4 GeV, taken during the year 2004 & 2005 are presented in this paper. Only minimum bias events are taken for this analysis which was obtained by coincidence between two Zero Degree Calorimeters (ZDCs) and a minimum signal from Central Trigger Barrel (CTB). Events which were produced within  $\pm 50$  cm of the center of the TPC along the beam axis were accepted for analysis. The centrality determination of this analysis uses the multiplicity of charged particles in the pseudorapidity range  $|\eta| < 0.5$ , as measured by TPC.

Fig. 3 shows the measured pseudorapidity distributions for photons for several centrality classes in Cu + Cu collisions at  $\sqrt{s_{NN}} = 62.4$  GeV. For comparison HIJING predictions are also displayed in the figure. Fig. 4 exhibits the pseudorapidity distributions for photons for different centrality in Cu + Cu collisions at  $\sqrt{s_{NN}} = 200$  GeV. It is seen that matching with HIJING is better towards the central events.

Fig. 5 shows  $\frac{dN_{\gamma}}{d\eta}$ , scaled by the number of participating nucleons for each centrality.

It is observed that  $\frac{dN_{\gamma}}{d\eta}$ , scaled by the number of participating nucleons, is independent of centrality. Fig. 6 shows the longitudinal scaling for photons at different energies and centralities. Here, we compare pseudorapidity distribution per participant pair for Au + Au central (0-5%) and peripheral (40-50%) events at  $\sqrt{s_{NN}} = 62.4$  GeV, for Cu + Cu central (0-10%) and peripheral (30-40%) events at  $\sqrt{s_{NN}} = 200$  GeV as a function of  $\eta - y_{beam}$ . The WA98<sup>13</sup> data at  $\sqrt{s_{NN}} = 17.3$  GeV and the UA5<sup>19</sup> data for p

at  $\sqrt{s_{NN}} = 540$  GeV are also displayed. We observe

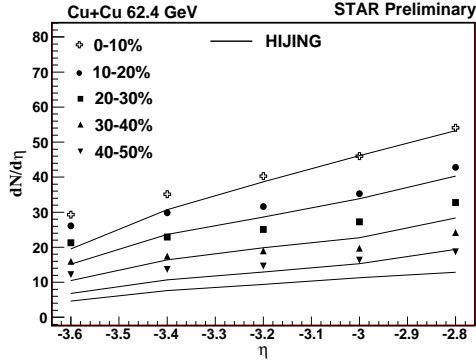


Fig. 3. Photons pseudorapidity density distribution,  $\frac{dN_\gamma}{d\eta}$ , measured for Cu + Cu at  $\sqrt{s_{NN}} = 62.4$  GeV. The statistical errors are within the symbol size.

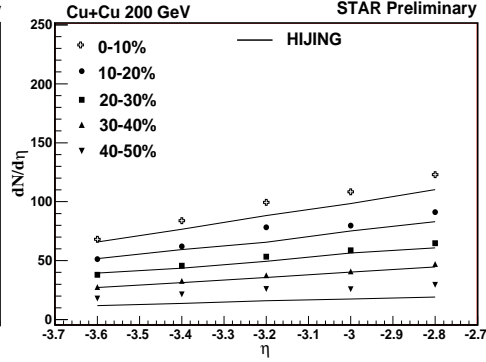


Fig. 4. Photons pseudorapidity density distribution,  $\frac{dN_\gamma}{d\eta}$ , measured for Cu + Cu at  $\sqrt{s_{NN}} = 200$  GeV. The statistical errors are within the symbol size.

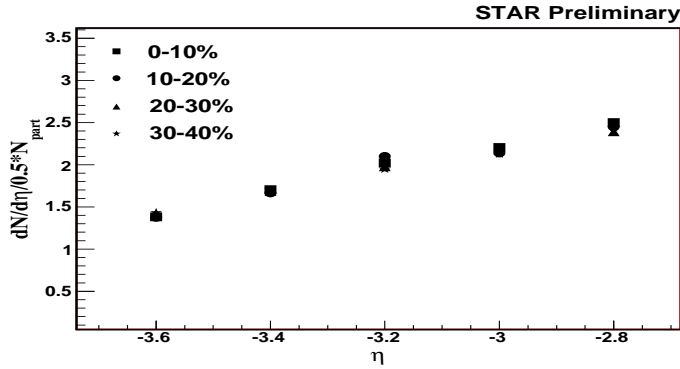


Fig. 5. Photons pseudorapidity distribution per participant pair,  $\frac{dN_\gamma}{d\eta} / 0.5 * N_{part}$ , measured for Cu + Cu at  $\sqrt{s_{NN}} = 200$  GeV for different centralities. The statistical errors are within the symbol size.

that photons follow universal limiting pseudorapidity distribution away from mid rapidity which is independent of energy, centrality and system size.

#### 4. Summary

The measurements of the pseudorapidity distributions from Cu + Cu collisions at top RHIC energy ( $\sqrt{s_{NN}} = 200$  GeV) and 62.4 GeV have been presented. Results have been compared with the HIJING Model. Photons pseudorapidity distributions follow limiting longitudinal scaling away from the mid rapidity. We further observe

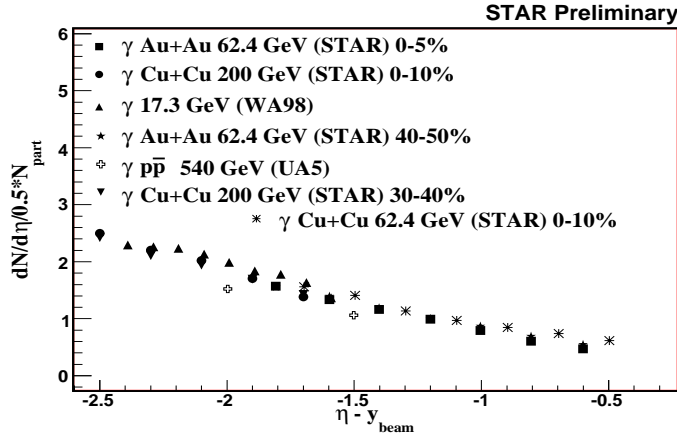
6 *Monika Sharma, Sunil Dogra, Neeraj Gupta*

Fig. 6. Photons pseudorapidity distribution per participant pair,  $\frac{dN_{\gamma}}{d\eta}$  as a function of  $\eta - y_{beam}$  for different energies & systems as indicated. The statistical errors are within the symbol size.

that longitudinal scaling is not only independent of energy but also independent of centrality and system size.

## References

1. F. Karsch Nucl. Phys. **A698** (2002) 199.
2. M. Biyajima *et al.*, Phys. Rev. Lett. B **515** (2001) 470-476.
3. J.J Marian, J. Phys. G, **30** (2004) S751-S758.
4. J.D. Bjorken, Phys. Rev. D **27** (1983) 140.
5. I.G. Bearden *et al.*, (BRAHMS Collaboration), Phys. Rev. Lett. **88** (2002) 202301, Phys. Lett. B **523** (2001) 227.
6. B.B. Back *et al.*, (PHOBOS Collaboration), Phys. Rev. Lett. **91** (2003) 052303, Phys. Rev. Lett. **87** (2001) 102303, Nucl. Phys. **A757** (2005) 28.
7. J. Adams *et al.*, (STAR Collaboration), Phys. Rev. C. **73** (2006) 034906.
8. M.M. Aggarwal *et al.*, (WA98 Collaboration), Phys. Rev. C. **65** (2002) 054912.
9. J. Adams *et al.*, (STAR Collaboration) Phys. Rev. Lett. **95** (2005) 062301.
10. M.M. Aggarwal *et al.*, (WA98 Collaboration), Phys. Rev. C. **64** (2001) 011901, Phys. Rev. Lett. B **403** (1997) 390-396, Phys. Rev. Lett. B **404** (1997) 207-212.
11. M.M. Aggarwal *et al.*, (WA98 Collaboration), Phys. Rev. Lett. **85** (2000) 3595.
12. K. J. Eskola Nucl. Phys. **A698** (2002) 78c.
13. M.M. Aggarwal *et al.*, (WA98 Collaboration), Phys. Lett. B. **458** (1999) 422.
14. J. Benecke *et al.*, Phys. Rev. **188** (1969) 2159.
15. B.B. Back *et al.*, arxiv:nucl-ex/0604017.
16. X.N. Wang and M. Gyulassy, Phys. Rev. D **44** (1991) 3501.
17. M.M Aggarwal *et al.*, Nucl. Instrum. Meth. A **499** (2003) 751-761.
18. V. Fine and P. Nevski, in proceedings of CHEP-2000, Padova, Italy.
19. K. Alpgard *et al.*, (UA5 Collaboration), Phys. Lett. B **115** (1982) 71; G.J. Alner *et al.*, Z. Phys. C **33** (1986) 1.